Nanostructures

DOI: 10.1002/ange.200503208

DNA-Templated Self-Assembly of Two-Dimensional and Periodical Gold Nanoparticle Arrays**

*Jaswinder Sharma, Rahul Chhabra, Yan Liu, Yonggang Ke, and Hao Yan**

Nanoparticles (NPs) are being actively developed as building blocks for electronic, photonic, and spintronics devices. When they are organized into well-defined ensembles, their collective properties depend critically on the interparticle spacings and their hierarchical organization. Up to now, methods to control these parameters were scarce. DNA-templated self-assembly provides a unique solution to meet the above challenge, largely because of the following features of DNA and DNA-based nanostructures: DNA has a well-defined geometry and highly predictable, diverse, and programmable intra/intermolecular interactions; DNA can be conveniently modified by different chemical groups, which act as linkers to covalently attach DNA oligomers to the surface of NPs; the design of stiff DNA-based nanostructures and their self-assembly have become a routine method to construct one- and two-dimensional DNA lattices of well-defined patterns.[1–10] More specifically, when NPs are assembled onto self-assembled DNA lattices, the periodicities and interparticle spacings defined by the DNA scaffolds can be readily adjusted, with nanometer spatial precisions. This level of precision provides exquisite control in the construction of rationally defined NP architectures.

Although the generic idea of using DNA to scaffold nanoelectronics was first proposed by Robinson and Seeman 18 years ago,[11] the development of self-assembled DNA nanoscaffolds to organize functional nanomaterials is still in the early stages. There has been a limited number of works reporting developments towards this goal and most of them are focused on the use of flexible and linear DNA as templates.[12–22] To achieve more predictable structural geometries of NP arrays, it is desirable to use more rigid DNA nanostructures as scaffolds to reduce the conformational flexibility. Recently Le et al.[23] used a double-crossover DNA tiling lattice to direct the assembly of 5-nm Au NPs

[*] J. Sharma,[+] R. Chhabra,[+] Dr. Y. Liu, Y. Ke, Prof. H. Yan
Department of Chemistry and Biochemistry and Biodesign Institute
Arizona State University
Tempe, AZ 85287 (USA)
Fax: (+1) 480-965-2747
E-mail: hao.yan@asu.edu

[+] These two authors contributed equally

[**] We thank Dr. Junping Zhang for helpful discussions. This study was supported by grants from the NSF (CCF-0453686, CCF-0453685) and a research grant from the Biodesign Institute at ASU to H.Y.

Supporting information for this article is available on the WWW under http://www.angewandte.org or from the author.

functionalized with multiple copies of T_{15} sequences. This investigation represents a breakthrough in the use of self-assembled 2D DNA nanostructures as scaffolding for nanoelectronic materials. However, the presence of multiple copies of the same DNA sequence on the NP surface requires first depositing the DNA lattice onto a solid substrate before assembly of the NPs on the DNA lattice. This approach is to prevent the possible cross-linking between multiple layers of DNA lattices mediated by the multiple T_{15} on a single Au NP. Greater precision in controlling the final structure of the NP lattices would require the use of NPs functionalized with a single DNA strand or NPs conjugated with different strands in a stoichiometrically controlled fashion. This functionalization is particularly important in the hierarchical organization of DNA-templated NP arrays.

Herein, we report the first assembly of 5-nm Au NPs functionalized with a single DNA strand on three different patterned structural templates which are constructed from self-assembled DNA tiles. We show that the periodicity and interparticle spacings of the NP nanoarrays can be precisely controlled through variation of the DNA-tile dimensions. In our strategy, the NP-conjugated strand first participates in the formation of a single DNA-tile structure, this Au-NP-bearing DNA tile was subsequently used to assemble with another DNA tile to form three different lattice structures, each with a well-defined periodical pattern.

We have developed a new DNA/NP conjugate system that allows Au NPs to be readily assembled onto a DNA tiling system. This novel system is amenable both to the DNA-tiling-lattice formation and the prevention of nonspecific aggregations between the Au NPs. This development paves the way for the assembly of more complex nanoparticle arrays on DNA nanoscaffolds for future device applications. Previously, there has been two ways to conjugate DNA with Au NPs: 1) one Au NP is linked with many DNA oligomers, as developed by Mirkin et al.[13] and 2) one Au NP is linked with only one DNA oligomer, as developed by Alivisatos and co-workers.[26] Au-NP/DNA conjugates prepared by the method of Mirkin can tolerate high salt concentrations (e.g., 1 mM Mg^{2+}), but it is difficult control the stoichiometry. Au-NP/DNA conjugates prepared by the method of Alivisatos has a well-defined stoichiometry and allows precise structural control, but the particle tends to irreversibly aggregate at high salt concentrations, especially in the presence of Mg^{2+} ions. Unfortunately, high salt concentration (e.g., Mg^{2+}) was proven to be necessary for DNA self-assembly using tiling structures. Therefore, the above two methods alone are not ideal for DNA-tiling-lattice templated organization; as a result, previous Au-NP assemblies were mostly based on linear DNA structures, and the use of 2D DNA lattices to organize nanoparticles was not very successful, though the idea was proposed more than 18 years ago. Herein, we solved this problem by first coating a Au NP with the desired DNA in a 1:1 ratio using the strategy of Alivisatos, then further coating the Au NP with an excess of nonrelated DNA (thiolated T_5 oligomer) using the method of Mirkin. The resultant DNA/Au NP has advantages from both methods: a well-defined stoichiometry and a resistance to high salt concentrations. The new DNA/Au NPs made it possible to program Au NPs into different architectures.

Figure 1 illustrates the design strategy and the three different lattice structures. A detailed description of the construction of DNA-tile structures and lattices can be found elsewhere.[24] In brief, the design of DNA nanostructures

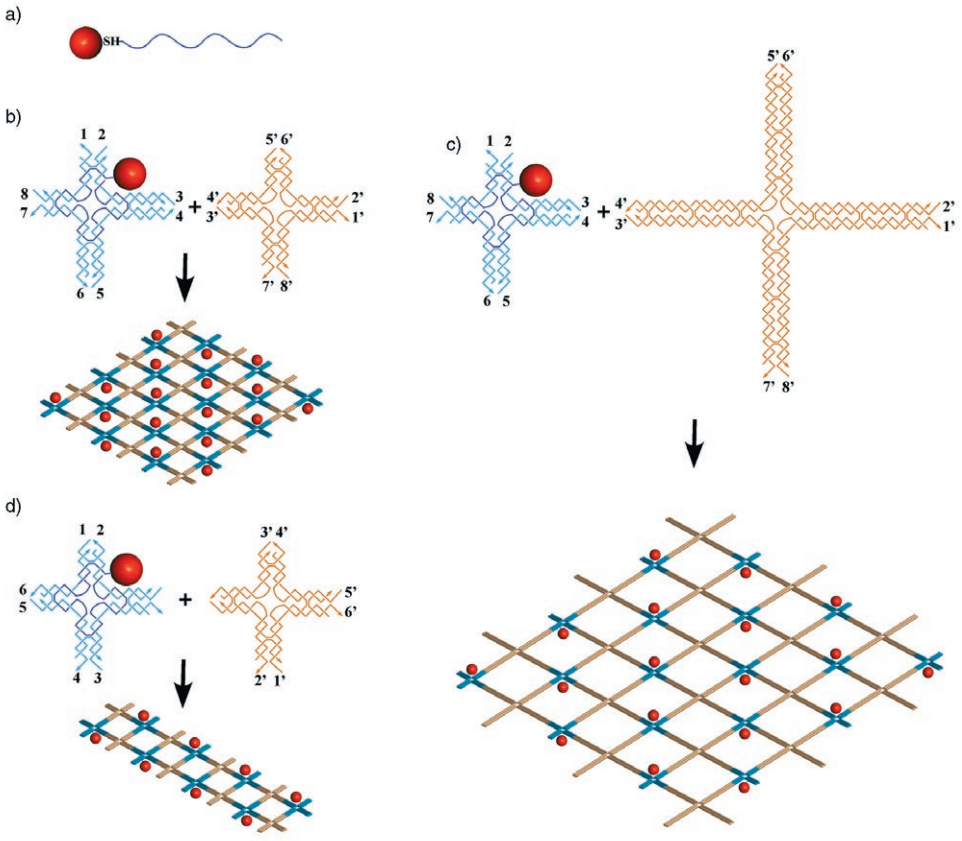

Figure 1. Schematic representations of the DNA-templated assembly of periodical Au-NP nanoarrays. a) A 1:1 conjugate of a Au NP (red ball) with a thiolated DNA strand (dark-blue curved line). b) A Au NP on a NGAB lattice. The DNA strands self-assemble into the cross-shaped A (blue) and B (orange) tiles with sticky ends so that 1 is complemented with 1′, 2 with 2′, and so forth. The central strand on A tile carries the Au NP into the self-assembled 2D nanogrid. c) A Au NP on a NGABL lattice. The A tile remains the same as in (b), and the four arms of the B tiles are each elongated by four DNA helical turns, thus the 2D arrays assembled have a larger cavity. d) A Au NP on a NTAB lattice. They self-assemble into 1D nanotrack by modifying the sticky ends of the A and B tiles. Note: all the A tiles share the same central strand that carries the Au NP.

begins with the self-assembly of a set of single-stranded DNA molecules into branched motifs known as tiles. DNA tiles carry single-stranded overhangs, or "sticky ends", which are encoded to recognize the complementary sticky ends of other DNA tiles, thus facilitating their self-assembly into ordered lattices. Herein, we utilize a family of DNA tiles that resemble a cross structure composed of four four-arm DNA branch junctions to template the assembly of Au NPs. A single unit of the cross structure has been shown to self-assemble into 2D nanogrids that display periodic square cavities.[5] A two-tile system (A and B tiles) has also been developed so that A and B tiles associate with each other alternatively to form 2D nanogrids or 1D nanotracks.[25] Herein, we utilize the A/B tile system and link the 5-nm Au NPs (represented as a red ball) with a 109-base-DNA strand (colored bright blue) that participates in the A tile (colored blue). The A and B tiles and their sticky ends are designed so that they can form three different lattice structures, as illustrated in Figure 1 b–d, respectively. The distance between neighboring A and B tiles in Figure 1 b is 4.5 helical turns of DNA, and the dimension of each cavity from center to center measures approximately 19.3 nm (this lattice structure is termed "NGAB"). We added an extra four turns to each arms of the B tile in Figure 1 c so that the dimension of the cavity becomes larger and measures approximately 33 nm (this lattice structure is termed "NGABL"). Figure 1 d illustrates that a nanotrack can be formed from the A and B tiles used in Figure 1 b by redesigning the sticky-ends matching strategy and blocking the growth of the lattice along the second dimension (this lattice structure is termed "NTAB"). In our design, the Au-NP-conjugated DNA strand participates in the A tile, weaving through the four arms of the cross with an extra T9 region that protrudes out from the side of the tile to prevent potential steric hindrance between the Au NP and the tile itself. The arrangements of the DNA tiles and the relative positions of the Au NPs on the three different DNA lattices are illustrated in Figure 1 as 3D side views. Note that there are relative rotations (in plane rotation and/or flipping over) of the A tiles, thus the positions of the Au NPs within the lattice cavities are controlled and well defined. Detailed schematic representations that show such rotations can be found in the Supporting Information. Overall, the above design provides us an excellent platform to test the DNA/nanostructure templated assembly of Au NPs and the control of interparticle spacings determined by their underneath lattices.

To achieve the above design, we adopted reported methods[26] to first conjugate the 109-base thiolated DNA strand in the A tile (which is shown as the dark-blue strand in Figure 1) to the surface of the 5-nm Au NPs, and the Au NP that contains a single copy of the DNA strand was isolated with 3% agarose gel electrophoresis (see the Experimental Section). Figure 2 a is an agarose gel that shows the separation of Au NPs with different copies of DNA strands conjugated to it. The band that corresponds to the 1:1 ratio of the Au NPs and DNA migrates slower relative to the bare Au NPs and was purified out of the gel for further annealing with other DNA strands to form the A-tile structures shown in Figure 1.

Figure 2 b shows a native agarose gel that demonstrates that the 5-nm Au NP conjugated with a single DNA strand

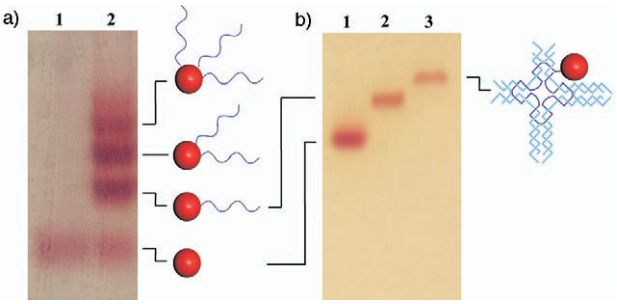

Figure 2. a) The Au NPs conjugated with different numbers of the thiolated ssDNAs are separated by 3% agarose gel electrophoresis. Lane 1: Au NP alone; lane 2: a mixture of Au NP with the thiolated DNA strands. The ratios between Au and DNA for each band are indicated at the side. b) The incorporation of the Au NP into the A tile is confirmed by using 3% native agarose gel. Lane 1: Au NP alone; lane 2: 1:1 conjugate of a Au NP with the 109-base-DNA strand; lane 3: annealed A tile carrying one Au NP.

participates in the formation of the A-tile structure, thus allowing a single Au NP to be incorporated in the tile. Lane 1 contains the 5-nm Au NP with no DNA attached. Lane 2 contains a Au NP conjugated with a single 109-base-DNA strand obtained from the separation protocol shown in Figure 2 a. Lane 3 contains the annealed A tile that is composed of the DNA strand conjugated with a Au NP and all the other strands involved in the A tile. A single and slower migrating pink band relative to the band in lane 2 indicates the successful incorporation of the 5-nm Au NP into the A tile.

It is important to point out again that we have optimized the buffer conditions to be amenable to the formation of the tile structure and also prevent the aggregation of Au NPs. We have observed that the 5-nm Au NPs and their DNA conjugates have the tendency to precipitate when there are Mg^{2+} ions (>1 mM) present in the buffer. However, the presence of Mg^{2+} ions (>1 mM) is usually required for the proper hybridization of the DNA-base pairing in the formation of the DNA-tile structures and lattices. To solve this problem, we replaced the Mg^{2+} ions with a higher concentration of Na^{+} ions in a TBE buffer (Tris–borate ethylenediaminetetraacetic acid (EDTA); 89 mM Tris, 89 mM boric acid, 2 mM EDTA, and 600 mM sodium chloride, pH 8.0). We found that under this buffer condition the A/B tile used can form 2D nanogrids and 1D nanotracks, but the 5-nm Au NPs conjugated with DNA form aggregates. We added thiolated short T5 oligomers to cover the surface of the Au NPs and further stabilize and prevent aggregation between the Au NPs. This approach greatly increases the charge density of the Au-NP surface, thus Au NPs with the thiolated T5 oligomers do not aggregate in 600 mM NaCl buffer.

After the Au NPs conjugated with the 109-base-DNA strand were incorporated into the A tile, the A tiles were mixed with three different B tiles to further self-assemble into the NGAB, NGABL, and NTAB lattices (Figure 1 b–d). The Au-NP lattices formed by the templated assembly were deposited onto the mica surface and observed by atomic force microscopy (AFM). Figure 3 a–c shows AFM images that correspond to the NGAB, NGABL, and NTAB lattice

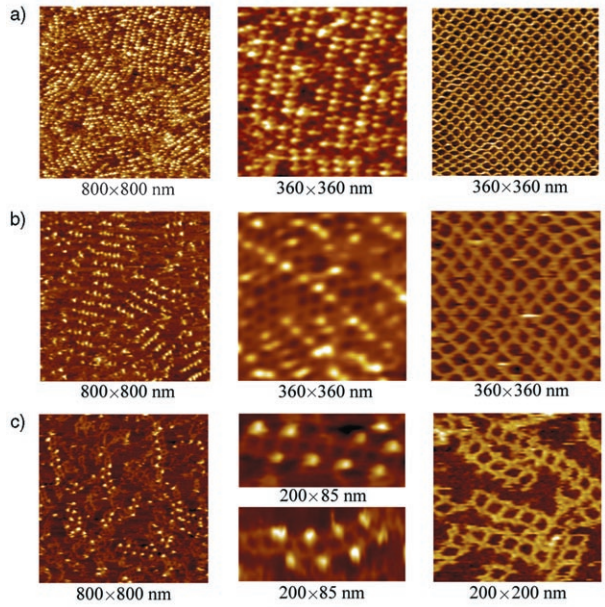

Figure 3. AFM images show the patterning of Au NPs on the self-assembled DNA nanostructures. a) Au NPs on NGAB lattices; b) Au NPs on NGABL lattices; c) Au NPs on NTAB lattices. In each group of images, the right image shows the DNA lattice or arrays without the Au NPs. The height scales for these images are approximately 2 nm. The images on the left are large scan areas that show the regular patterning of AU NPs. The middle images are zoom-in, high-resolution scans which show both the Au NPs and the DNA scaffolds underneath. The height scales for these images are approximately 5 nm.

structures, respectively. The left panels in Figure 3 a–c show a larger scan area, followed by the zoom-in image for a close-up view of both the NPs and their underlying DNA nanogrids and nanotracks. The panels on the right are images that show the control experiments when the Au NPs were not attached to the 109-base-DNA strand. The Au NPs appear as brighter dots with heights measuring 4.3–5.1 nm (Figure 4). The AFM images reveal periodical NP-lattice structures for each design, and the measured repeating distance between the particles are shown in Figure 4, which match the designed parameters. The underlying DNA lattices are revealed clearly in the zoom-in images. The enlargements of the particle–particle distances shown in Figure 3 b confirmed the designed increase in the helical turns between the A and B tiles. The resolution obtained for the zoom-in image shown in Figures 3 c and 4 b can even tell the exact position of the Au NPs relative to each individual tile, thus matching the designed pattern illustrated in Figure 1 c, d (detailed analysis of these patterns is shown in the Supporting Information).

It is notable that the DNA lattices underneath the NPs observed by AFM do not show a perfect square most of the time, but rather a rhombus shape. The flexibility of the cross-shaped tile at the crossing point has been recognized in the bare DNA 2D array formed, in which the acute angle of the cross may range from 90° to as small as 45° under stress. It is also noted that the NPs are always positioned at the corner of the crossing with the obtuse angle. The formation of the obtuse angle at the corner containing the NP possibly results from positioning the NPs at the crossing, which induces steric displacement in the DNA helices, or from the electrostatic repulsion between the highly negative charged NP (with multiple copies of T5 strands on surface) and the DNA bases in the phosphate backbone of the DNA strand. The rhombus-shaped cavity led to a shortened distance between the NPs along one diagonal direction and an elongated distance along the other diagonal direction.

The well-defined periodicity and the AFM image and profile clearly demonstrated that the NPs are sitting on the DNA lattices in a rationally organized fashion. However, it is also noted that there are some tiles in the A-tile position on the DNA lattice lacking the Au NPs. We reasoned that this positioning is because the Au NP and DNA linkage is not strong enough, so some Au NPs become detached from the DNA strands in the processing procedures after the gel-

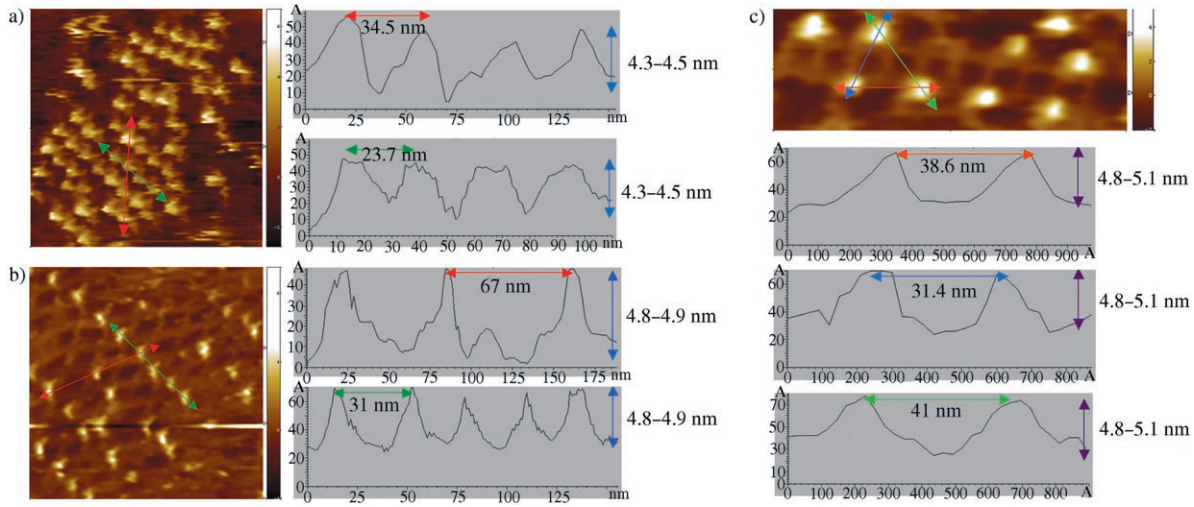

Figure 4. Surface cross-section analysis of the AFM images. a) Au NPs on a NGAB lattice; b) Au NPs on a NGABL lattice; c) Au NPs on a NTAB lattice. The lines with a double arrowhead in the images indicate the range of the cross-section analysis. Their colors correspond to the colors of the arrows on the profile plots. Distance and height measured are labeled in the profile plots. The measured distances are all within ±2 nm to the calculated distances from the design.

purification step. The DNA strand lacking the Au NP still can be incorporated into the A tile and then grow into the DNA lattice in the following annealing steps. Stable linkages between the DNA strands and NPs need to be developed to achieve a higher yield of the NP assembly on the DNA nanoscaffolds.

In summary, we have successfully demonstrated the incorporation of a single Au NP into an unique rationally designed DNA-nanostructural building block (an unit tile), and used the NP-bearing DNA tile for the directed self-assembly of two-dimensional NP arrays with well-defined periodical patterns and precisely controlled interparticle spacings. This approach opens up great opportunities to control the interparticle spacings and hierarchical architectures of nanoparticles. With the development of DNA nanotechnology, the design of DNA-nanostructural building blocks of different geometries and lattice morphologies is not a formidable task any more. By introducing unique sticky ends to the NP-bearing DNA building blocks, sophisticated patterns can be achieved, opening up opportunities to construct useful nanoscale devices from the well-organized nanoparticles. For example, photonic antenna could be constructed by aligning metallic nanoparticles of different sizes into a chain or parallel chainlike configuration with well-defined interparticle spacings.[27] Precisely controlled organization of Au and other nanoparticles onto patterned DNA lattices could also enable us to study their distance-dependent optical and electronic properties. To maximize the full potential of using DNA nanoarchitecture to scaffold nanoelectronics, it is necessary to develop methods to assemble other type of NPs, such as magnetic, semiconductor NPs onto DNA templates.

Experimental Section

DNA-tile complex and lattice formation: The sequences of all DNA strands used are listed in the Supporting Information. The DNA sequences were designed with the SEQUIN program.[28] DNA strands were synthesized by Integrated DNA Technologies, Inc. (www.idtdna.com) and purified by denaturing polyacrylamide gel electrophoresis (PAGE). DNA-tile complexes (A and B tiles) were formed by mixing an equal quantity of each strand designed in the complex at a concentration of 1 μM, as estimated by OD_{260}, in 1 × TBE/Na^+ buffer (89 mM Tris, 89 mM boric acid, 2 mM EDTA, and 600 mM sodium chloride, pH 8.0).

Phosphination of Au NPs: Au colloids with diameters of 5 nm (purchased from Ted Pella Inc.) were stabilized by complexation with bis(*p*-sulfonatophenyl)phenylphosphine dihydrate dipotassium salt (Strem Chemicals Inc.). This salt (20 mg) was added to the gold-colloid solution (100 mL; ≈1 OD at 520 nm), the mixture was shaken overnight at room temperature. NaCl (solid) was then added slowly to this mixture while stirring until the color changed from deep burgundy to light purple. The supernatant was carefully removed with a pipette after centrifugation, and the Au NPs were resuspended in 1 mM phosphine solution (5 mL). Methanol (5 mL) was added, the mixture centrifuged, the supernatant removed, and the Au NPs were resuspended in 2.5 mM phosphine solution (2 mL). The concentration of the Au NPs was estimated from the optical absorbance at 520 nm. Phosphine coating gives a net negative charge on the particle surface, which stabilizes the Au NPs in high concentrations of particles and electrolytes.

Au/DNA conjugates: The thiolated DNA strand was purchased from IDT and purified by denaturing PAGE. The thiolated DNA strand was incubated overnight with Au NPs capped with phosphine in a ratio of 1.0:1.0 in 0.5 × TBE containing 50 mM NaCl at room temperature. Different combinations of DNA/Au conjugates (particles bearing 1–4 single-stranded DNAs (ssDNAs)) were separated by 3% agarose gel (running buffer 0.5 × TBE, loading buffer 30% glycerol, at 15 $V\,cm^{-1}$). Different bands were clearly visible from the red color of the Au NPs. The band with DNA/Au in a 1:1 ratio was electro-eluted onto the glass fiber filter and a dialysis membrane (MWCO 10000) inserted in front of the band in the gel. The conjugate was recovered using a 0.45-μm centrifugal filter device. The concentration of this Au NP/DNA conjugate was estimated from the optical absorbance at 520 nm.

Further stabilization of Au NPs: The Au particles conjugated with the 109-base-DNA strand were further stabilized by adding thiolated T5 ssDNA oligomers to avoid further coagulation during annealing under high-electrolyte conditions. This stabilization was carried out by incubating a relatively high concentration (T5/Au = 100:1) of ssDNA T5 relative to the concentration of DNA/Au conjugates in 0.5 × TBE buffer containing 50 mM NaCl overnight at room temperature.

Au-NP and DNA-tile assemblies: To form the A-tile structure bearing a single 5-nm Au NP, the Au NP conjugated with the 109-base-DNA strand was heated at 60 °C for 5 min. The other strands of the A tile were also preheated at 90 °C for 5 min. These two solutions were mixed together at 60 °C in an equimolar ratio and were slowly cooled to room temperature in 1 × TBE buffer containing 600 mM NaCl. Another tube contained annealed strands comprising the B tile in 1 × TBE containing 600 mM NaCl. The A and B tiles annealed separately were mixed in 1:1 ratio at 40 °C and cooled slowly to room temperature. Similar procedures were adopted for the NGABL and NTAB systems.

AFM imaging: A mixture of 1 × TAE/Mg (2 μL; 40 mM Tris, 20 mM acetic acid, 2 mM EDTA, 12.5 mM magnesium acetate, pH 8.0) buffer was first dropped onto freshly cleaved mica (Ted Pella, Inc.) and left to adsorb onto the surface for 2 min. A sample of the DNA lattice (2 μL) was deposited on the drop. Mg preadsorbed on mica can help the DNA structure stay on the mica during the AFM scan. Buffer (1 × TAE/Mg; 400 μL) was added to the drop on the mica and imaging was performed in a fluid cell in AAC mode on a Pico-plus atomic force microscope (Molecular Imaging) using NP-S tips (Veeco Inc.).

Received: September 9, 2005
Published online: December 19, 2005

Keywords: DNA · nanoparticles · nanostructures · scanning probe microscopy · templated self-assembly

[1] N. C. Seeman, *Nature* **2003**, *421*, 427 – 431.
[2] E. Winfree, F. Liu, L. A. Wenzler, N. C. Seeman, *Nature* **1998**, *394*, 539 – 544.
[3] T. H. Labean, H. Yan, J. Kopatsch, F. R. Liu, E. Winfree, J. H. Reif, N. C. Seeman, *J. Am. Chem. Soc.* **2000**, *122*, 1848 – 1860.
[4] C. D. Mao, W. Q. Sun, N. C. Seeman, *J. Am. Chem. Soc.* **1999**, *121*, 5437 – 5443.
[5] H. Yan, S. H. Park, G. Finkelstein, J. H. Reif, T. H. LaBean, *Science* **2003**, *301*, 1882 – 1884.
[6] P. W. K. Rothemund, N. Papadakis, E. Winfree, *PLoS Biol.* **2004**, *2*, 2041 – 2053.
[7] B. Q. Ding, R. J. Sha, N. C. Seeman, *J. Am. Chem. Soc.* **2004**, *126*, 10230 – 10231.
[8] J. C. Mitchell, J. R. Harris, J. Malo, J. Bath, A. J. Turberfield, *J. Am. Chem. Soc.* **2004**, *126*, 16342 – 16343.
[9] N. Chelyapov, Y. Brun, M. Gopalkrishnan, D. Reishus, B. Shaw, L. Adleman, *J. Am. Chem. Soc.* **2004**, *126*, 13924 – 13925.

[10] Y. He, Y. Chen, H. Liu, A. E. Ribbe, C. Mao, *J. Am. Chem. Soc.* **2005**, *127*, 12202 – 12203.
[11] B. H. Robinson, N. C. Seeman, *Protein Eng.* **1987**, *1*, 295 – 300.
[12] For a recent review on this topic, see: C. M. Niemeyer, U. Simon, *Eur. J. Inorg. Chem.* **2005**, *18*, 3641 – 3655.
[13] C. A. Mirkin, R. L. Letsinger, R. C. Mucic, J. J. Storhoff, *Nature* **1996**, *382*, 607 – 609.
[14] A. P. Alivisatos, K. P. Johnsson, X. Peng, T. E. Wilson, C. J. Loweth, M. P. Bruchez, Jr., P. G. Schultz, *Nature* **1996**, *382*, 609 – 611.
[15] C. J. Loweth, W. B. Caldwell, X. Peng, A. P. Alivisatos, P. G. Schultz, *Angew. Chem.* **1999**, *111*, 1925 – 1929; *Angew. Chem. Int. Ed.* **1999**, *38*, 1808 – 1812.
[16] C. M. Niemeyer, W. Bürger, J. Peplies, *Angew. Chem.* **1998**, *110*, 2391 – 2395; *Angew. Chem. Int. Ed.* **1998**, *37*, 2265 – 2268.
[17] H. Li, S. H. Park, J. H. Reif, T. H. LaBean, H. Yan, *J. Am. Chem. Soc.* **2004**, *126*, 418 – 419.
[18] P. Hazarika, B. Ceyhan, C. M. Niemeyer, *Angew. Chem.* **2004**, *116*, 6631 – 6633; *Angew. Chem. Int. Ed.* **2004**, *43*, 6469 – 6471.
[19] Z. Deng, Y. Tian, S. Lee, A. E. Ribbe, C. Mao, *Angew. Chem.* **2005**, *117*, 3648 – 3651; *Angew. Chem. Int. Ed.* **2005**, *44*, 3582 – 3585.
[20] S. A. Claridge, S. L. Goh, J. M. Frechet, S. C. Williams, C. M. Micheel, A. P. Alivisatos, *Chem. Mater.* **2005**, *17*, 1628 – 1635.
[21] B. Zou, B. Ceyhan, U. Simon, C. M. Niemeyer, *Adv. Mater.* **2005**, *17*, 1643 – 1647.
[22] R. Kretschmer, W. Fritzsche, *Langmuir* **2004**, *20*, 11797 – 11801.
[23] J. D. Le, Y. Pinto, N. C. Seeman, K. Musier-Forsyth, T. A. Taton, R. A. Kiehl, *Nano Lett.* **2004**, *4*, 2343 – 2347.
[24] N. C. Seeman, *Methods Mol. Biol.* **2005**, *303*, 143 – 166.
[25] S. H. Park, P. Yin, Y. Liu, J. H. Reif, T. H. LaBean, H. Yan, *Nano Lett.* **2005**, *5*, 729 – 733.
[26] D. Zanchet, C. M. Micheel, W. J. Parak, D. Gerion, A. P. Alivisatos, *Nano Lett.* **2001**, *1*, 32 – 35.
[27] K. Li, M. T. Stockman, D. J. Bergman, *Phys. Rev. Lett.* **2003**, *91*, 227402 – 227402:1 – 4.
[28] N. C. Seeman, *J. Biomol. Struct. Dyn.* **1990**, *8*, 573 – 581.

